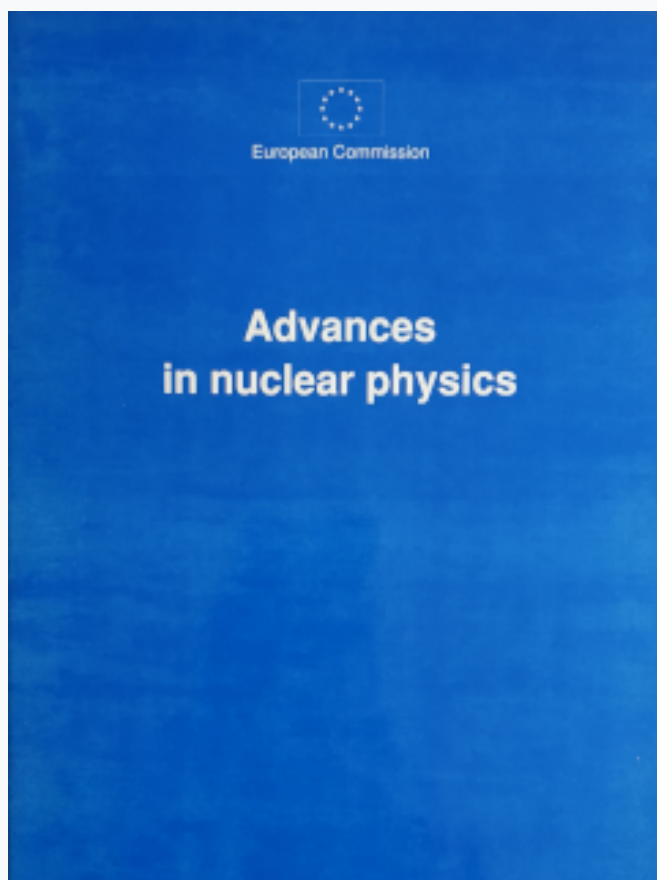


HNPS Advances in Nuclear Physics

Vol 5 (1994)

HNPS1994



Shell model calculations in the A=90-98 mass region. A study of the N=51. nuclei

P. Divari, L. D. Skouras

doi: [10.12681/hnps.2895](https://doi.org/10.12681/hnps.2895)

To cite this article:

Divari, P., & Skouras, L. D. (2020). Shell model calculations in the A=90-98 mass region. A study of the N=51. nuclei. *HNPS Advances in Nuclear Physics*, 5, 90–103. <https://doi.org/10.12681/hnps.2895>

Shell model calculations in the $A=90-98$ mass region.
A study of the $N=51$ nuclei.

P. Divari and L.D. Skouras

¹Institute of Nuclear Physics, NCSR *Demokritos*, GR-15310 Aghia Paraskevi,
Attiki, Greece

Abstract

The properties of nuclei with $39 \leq Z \leq 47$ and $N = 51$ are investigated in large scale shell-model calculations. The doubly closed nucleus $^{100}_{50}\text{Sn}$ is selected as the reference state and the nuclei under examination are described in terms of proton holes and a single neutron outside the inert core. The proton holes are distributed in a model space consisting of the orbitals $g_{9/2}$, $p_{1/2}$, $p_{3/2}$ while $f_{5/2}$ is sometimes also considered. Similarly the model space for the single neutron includes the orbitals $g_{7/2}$, $d_{5/2}$, $d_{3/2}$, $s_{1/2}$ and in certain cases $h_{11/2}$. The effective two-body interaction and the matrix elements of the effective operators were determined by introducing second-order corrections to the Sussex matrix elements. The single proton holes as well as the single-neutron energies were treated as parameters which were determined by least-squares fit to the observed levels of $39 \leq Z \leq 47$, $N = 50$ and $N = 51$ respectively. The results of the calculation were found to be in satisfactory agreement with experimental data and this enable us to make predictions about the properties of some exotic nuclei in the vicinity of ^{100}Sn .

1 Introduction

With the development of new experimental techniques it has become possible to study the very proton-rich nuclei. Studies of the $^{98}_{51}\text{Ag}$, $^{99}_{51}\text{Cd}$ and $^{100}_{50}\text{Sn}$ should be available in the near future. The experimental study of nuclei in the vicinity of $^{100}_{50}\text{Sn}$ provides a nice area for comparisons with nuclear structure models. Because the 50 protons and 50 neutrons correspond to a well-established shell closure, it is convenient to use the doubly closed nucleus $^{100}_{50}\text{Sn}$ as the closed inert core and study configurations with few particles and holes outside of it. So the effects of variation of the model space can be studied systematically.

Talmi and Unna¹) made the first treatment of the $N = 50$ nuclei in 1960. They determined effective interaction within a model space $g_{9/2}$ and $p_{1/2}$ by least-squares

¹Presented by P. Divari

fit to the then known experimental energy levels. Several other shell model studies of nuclei $Z, N \leq 50$ followed the work of Talmi and Unna. Gazzaly²⁻³⁾ *et al* studied ^{90}Zr in the extended model space $g_{9/2}, p_{1/2}, p_{3/2}$ and $f_{5/2}$ assuming $^{78}_{28}\text{Ni}$ as core and using an empirical interaction. The approach of Gazzaly *et al* has been adopted by Ji and Wildenthal in their studies⁴⁻⁶⁾ on the properties of the $N = 50$ nuclei. Recently successful theoretical investigations⁷⁻¹⁰⁾ on the mass region $A = 80 - 100$, were realized in a model space consisting of the $g_{9/2}, p_{1/2}, p_{3/2}$ and $f_{5/2}$ proton and neutron hole orbitals outside the doubly-closed core $^{100}_{50}\text{Sn}$. The wavefunctions of those calculations were used to determine the double β decay of Ge, Se, Sr and Kr isotopes. Skouras and Dedes¹¹⁾ made also an attempt to explain the observed even-parity spectrum and transitions rates of ^{95}Tc . In this shell-model approach three valence protons were restricted to the $g_{9/2}$ orbital, while full configuration mixing has been assumed for the two valence neutrons which are allowed to take all possible values in the $d_{5/2}, d_{3/2}, s_{1/2}$ and $g_{7/2}$ orbitals. Despite the success these calculations have had their model space for the valence proton particles was very restricted for the description of nuclei with $Z \geq 38$, specially for the nuclei in the middle of the proton shell.

In this work¹²⁾ an attempt is made to explain the energy spectra and the decay properties of nuclei $39 \leq Z \leq 47, N = 51$. Our calculation differs from the previously mentioned shell-model calculation of Skouras and Dedes in respect of full configuration mixing between protons is allowed. For this reason the nucleus ^{100}Sn is selected as the inert core outside of which proton-holes and a single-neutron are distributed in two separate model spaces. The determination of effective two-hole as well as particle-hole interactions are evaluated in a realistic way. Details of the model spaces we consider are discussed in sec. 1 while the results of the calculation are presented in sec. 2.

2 Details of the calculation

The shell-model Hamiltonian which describes the nuclei $39 \leq Z \leq 47$ and $N = 51$ can be expressed as the sum of three terms

$$H = H_h + H_p + V_{hp} \quad (1)$$

where H_h and H_p denote the Hamiltonians in the proton and neutron spaces respectively, while V_{hp} represents the interaction between proton-holes and the neutron-particle. Each of the H_h and H_p terms consists of a single-particle and a two-body

term, although the two-body part of H_p does not enter in the present study of the $N = 51$ nuclei.

The basis vectors for a weak-coupling calculation have the form

$$|(n_h \mu_h j_h^{-1}), j_p; J\rangle \quad (2)$$

where $|n_h \mu_h j_h^{-1}\rangle$ denotes the proton hole wave functions. The index n_h denotes the number of protons while μ_h distinguishes the orthogonal states which all correspond to the same j_h value. So the first step for the construction of H is the determination of H_h Hamiltonian⁷⁻⁸).

For this reason we consider the nucleus $^{100}_{50}\text{Sn}$ as the inert core placing in principle proton holes in the model space consisting of the orbitals $g_{9/2}$, $p_{1/2}$ and $p_{3/2}$. After systematic analysis it was found that this model space was not so realistic for the description of nuclei in the middle of the proton shell since, the presence of the $f_{5/2}$ within the model space gives rise to strong configuration mixing. So we have considered two model spaces. The model space $g_{9/2}$, $p_{1/2}$, $p_{3/2}$, hereafter to be referred to as mod1, quite realistic for the description of the nuclei $42 \leq Z \leq 47$ and another one consisting of the orbitals $g_{9/2}$, $p_{1/2}$, $p_{3/2}$ and $f_{5/2}$ referred as mod2, proper for the investigation of the nuclei $39 \leq Z \leq 41$. The determination of H_h demands the

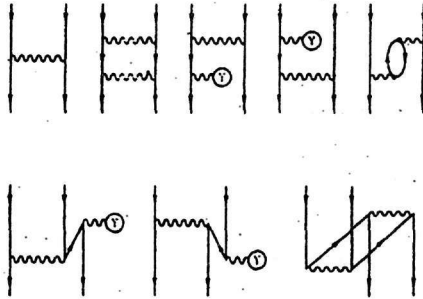


Figure 1: Diagrams considered in the determination of the two-hole effective interaction calculation of the two-body effective interaction. This is realized by perturbation theory introducing second order corrections, in a space of $2\hbar\omega$ excitations above the model space. The NN interaction we consider is the Sussex¹³) potential, while the diagrams we computed are shown in fig 1. The basic assumption of our calculation

is that we use harmonic oscillator potential as the zero-order single-particle spectrum, for which the oscillator parameter $b = (\hbar/m\omega)^{1/2}$ has been given the value 2.1 fm appropriate for this mass region. In table 1 we list a selection of matrix elements of the two-body effective interaction for the model spaces mod1 and mod2.

Table 1

Matrix elements $\langle j_1^{-1} j_2^{-1}; J | V | j_3^{-1} j_4^{-1}; J \rangle$ (in MeV)
for proton-holes in the model spaces mod1 and mod2

$2j_1$	$2j_2$	$2j_3$	$2j_4$	J	mod1	mod2
9	9	9	9	0	-1.4872	-1.5090
				2	-0.7134	-0.7888
				4	-0.2088	-0.2111
				6	-0.0345	0.0099
				8	0.0905	0.1430
9	9	1	1	0	0.9346	0.9313
9	9	1	3	2	-0.3546	-0.3432
9	9	3	3	0	1.2870	1.3193
				2	0.4011	0.4381
9	1	9	1	4	0.0570	0.0919
				5	-0.4269	-0.4088
9	1	9	3	4	0.1246	0.1460
				5	-0.4340	-0.4678
9	3	9	3	3	-0.8119	-0.8734
				4	-0.0158	0.0139
				5	-0.1172	-0.0776
				6	0.1193	0.1705
1	1	1	1	0	-0.1476	-0.1421
1	1	3	3	0	-1.4767	-1.4936
1	3	1	3	1	0.1850	0.2354
				2	-0.7612	-0.7338
1	3	3	3	2	0.5872	0.5988
3	3	3	3	0	-1.2370	-1.2016
				2	-0.4374	-0.3976

As we can see the effects of $f_{5/2}$ orbit on the renormalization of the mod1 interaction are, in second order, very small.

The single hole-energies can not be taken from experiment, since the nucleus ${}^{99}_{50}\text{Sn}$ is far from the stability line, so they are treated as parameters which are determined

making a least-squares fit to the observed energy levels. Specifically we made two fitting procedures. The first includes nuclei from the mass region $42 \leq Z \leq 47$, $N = 50$ and the second one the nuclei $39 \leq Z \leq 41$, $N = 50$. Under these circumstances two sets of single-hole energies are obtained for the two model spaces we have considered. The first is

$$\epsilon_{9/2} = 0.00, \quad \epsilon_{1/2} = 1.21, \quad \epsilon_{3/2} = 2.18 \quad (3)$$

and the second one is

$$\epsilon_{9/2} = 0.00, \quad \epsilon_{1/2} = 1.80, \quad \epsilon_{3/2} = 3.30, \quad \epsilon_{5/2} = 6.28 \quad (4)$$

It is interesting to note comparing the above two sets of energies, that the additional $f_{5/2}$ orbital increases the energy of the $p_{1/2}$ state by about 600 KeV while the $p_{3/2}$ state by about 1 MeV. All the above single-particle energies have been computed with respect to $g_{9/2}$ orbital.

The single-neutron particle is placed in the model space consisting of the orbitals $g_{7/2}$, $d_{5/2}$, $d_{3/2}$ and $s_{1/2}$ but we have also examined the effects introduced by the inclusion of the $h_{11/2}$ within this model space. The small neutron model space will be referred as mod3 while the larger one as mod4. For the determination of the single-neutron energies we followed the same procedure as those for the proton holes. Namely we made a least-squares fit including available experimental data from the mass region $39 \leq Z \leq 47$, $N = 51$ into the fitting procedure. Having in mind that we treat two model spaces for the single-neutron, we can obtain two sets of single-particle energies.

$$\epsilon_{5/2} = 0.000, \quad \epsilon_{7/2} = 0.081, \quad \epsilon_{3/2} = 2.190, \quad \epsilon_{1/2} = 1.905 \quad (5)$$

and

$$\begin{aligned} \epsilon_{5/2} = 0.000, \quad \epsilon_{7/2} = -0.003 \quad \epsilon_{3/2} = 2.420, \quad \epsilon_{1/2} = 1.910 \\ \epsilon_{11/2} = 3.360 \end{aligned} \quad (6)$$

The additional $h_{11/2}$ orbital has little effect on the energies of the $s_{1/2}$ and $g_{7/2}$ but increases the energy of $d_{3/2}$ orbital by about 200 KeV.

Finally, the V_{hp} part of the shell-model Hamiltonian (1) has been determined, in the usual manner, by considering second-order corrections, in the space of $2\hbar\omega$ excitations, to the proton-hole, neutron-particle interaction.

In a similar manner to the perturbative determination of effective interaction, we have also determined the matrix elements of effective transition operators. As an example of this calculation we list in table 2 the reduced matrix elements corresponding to single-neutron particle states.

Table 2
matrix elements $\langle j_1 || T^L || j_2 \rangle^\dagger$ for neutron particles
in the model spaces mod3 and mod4

T^L	$2j_1$	$2j_2$	Bare	mod3	mod4
M1	7	7	2.3283	1.3182	1.3182
	7	5	0.	0.2295	0.2295
	5	5	-2.7052	-1.8573	-1.8573
	5	3	-2.8920	-3.9538	-3.9538
	3	3	1.4460	1.0194	1.0194
	3	1	0.	0.1042	0.1042
	1	1	-2.2863	-1.5775	-1.5775
	11	11	-3.5150		-2.5098
E2	7	7	0.	-12.581	-16.421
	7	5	0.	3.7737	4.1339
	7	3	0.	-10.033	-11.369
	5	5	0.	-7.5161	-8.9618
	5	3	0.	-3.7466	-4.6874
	5	1	0.	-6.2060	-7.4969
	3	3	0.	-5.6497	-7.0619
	3	1	0.	5.1973	6.2825
	11	11	0.		-13.300
M3	7	7	-96.533	-43.623	-47.987
	7	5	-57.035	-77.990	-88.559
	7	3	-49.394	-44.510	-49.874
	7	1	0.	-14.390	-23.055
	5	5	210.43	158.79	137.56
	5	3	114.54	140.93	153.65
	5	1	215.61	182.97	164.63
	3	3	-35.072	-33.901	-39.661
	11	11	271.26		179.40

[†]EL matrix elements are expressed in units of $e(fm)^L$ while ML in units $\mu_\nu(fm)^{(L-1)}$

Table 2
Continued

T^L	$2j_1$	$2j_2$	Bare	mod3	mod4
E4	7	7	0.	281.27	368.21
	7	5	0.	-183.62	-217.98
	7	3	0.	189.01	226.14
	7	1	0.	-195.54	-221.60
	5	5	0.	158.21	188.77
	5	3	0.	222.91	271.92
	11	11	0.		299.88
E3	7	11	0.		-32.874
	5	11	0.		75.305
M4	7	11	-1619.4		-915.47
	5	11	1536.3		1709.6
	3	11	-2410.4		-2273.5
M2	7	11	45.266		23.074
E5	7	11	0.		1041.7
	5	11	0.		-1190.7
	3	11	0.		874.67
	1	11	0.		-1109.5

In the first column we always obtain the values correspond to the bare operators. As we can see comparing the first column with the other two, the matrix elements are both sizable and state-dependent. On the contrary the reduced matrix elements in the two neutron model spaces mod3 and mod4 are quite similar. It is interesting to note that with the inclusion of $h_{11/2}$ within the neutron model space mod4, we can also describe the transitions M2, M4, E3 and E5.

3 Results of the calculation

In this section we present a selection of the results of our shell-model calculation on the $39 \leq Z \leq 47$, $N = 51$ nuclei and compare them with the experimental data.

If fig. 2 we can see the experimental and theoretical spectra of ^{97}Pd and ^{95}Ru . For these nuclei a detailed comparison with experiment is difficult due to the many uncertainties that still exist in the experimental spectra^{14,15}) even among the low-lying levels. Most experimental states up to 2.5 MeV of excitation are reproduced in

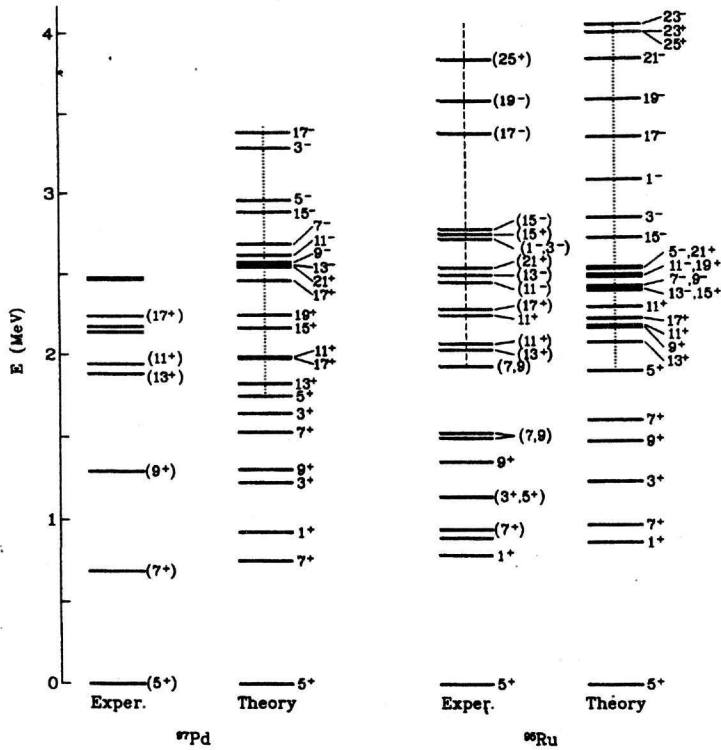


Figure 2: Theoretical and experimental spectra of ^{97}Pd and ^{95}Ru

the theoretical spectra within 100-200 KeV and in addition our calculation predicts the presence of several others. It is also interesting to note that in the spectrum of ^{95}Ru our calculation confirms the existence of some tentative high spin states that are above 2.5 MeV like the possible $15/2^-$, $17/2^-$, $19/2^-$ and $25/2^+$. We can also see observing the experimental spectra of ^{97}Pd and ^{95}Ru that there are levels for which no spin or parity assignments have been made. Until such assignments have been established the comparison between theory and experiment can not be complete.

Fig. 3 shows for comparison the theoretical and experimental spectra^{16,17)} of the nuclei ^{92}Nb and ^{94}Tc . For higher excitations the experimental knowledge of these two nuclei is still very incomplete and thus a detailed comparison between theory and experiment is not possible. Regarding the experimental spectra of ^{92}Nb generally there is good agreement between theory and experiment although there are many uncertainties to the experimental estimates specifically above 1 MeV. As we can see in the experimental spectrum of ^{92}Nb there is a 1^+ state at 1.08 MeV and a possible one at 0.97 MeV. The theoretical spectrum predicts only one such state at 0.63 MeV.

In fig. 4 is shown the spectra of ^{91}Zr and ^{93}Mo . Starting with the energy spectrum of ^{91}Zr we can see that all the energy levels are reproduced by our calculation to within

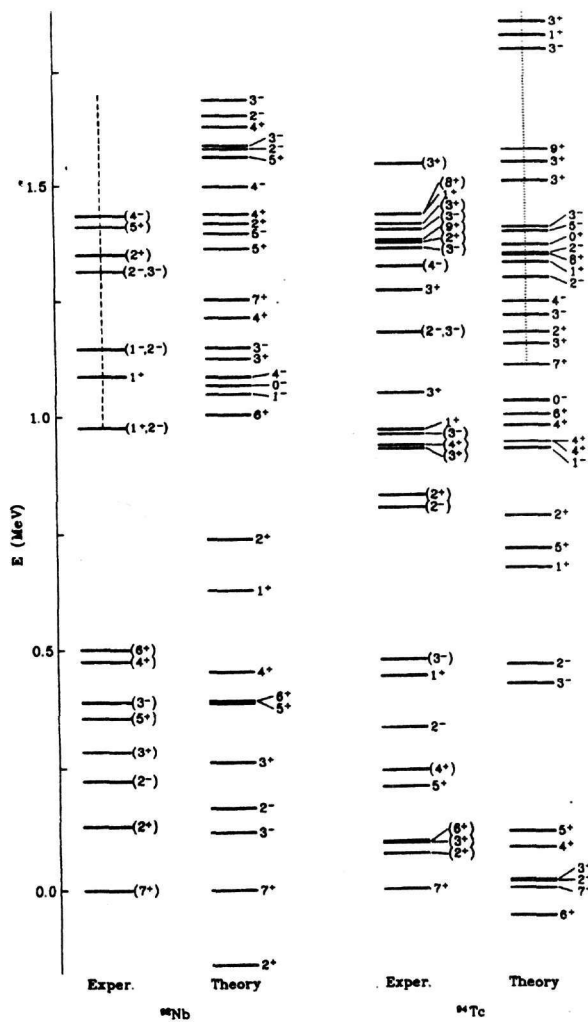


Figure 3: Theoretical and experimental spectra of ^{92}Nb and ^{94}Tc

100-400 KeV. There are some interesting features to be observed in this spectrum. i) Trying to describe the spectra of ^{91}Zr with the small model space of neutrons (mod3) the $11/2^-$ excited states are reproduced from 500 KeV up 1 MeV above the experimental ones¹⁸). The presence of $h_{11/2}$ orbital within the model space mod3 reproduces them to within 100 up 400 KeV of the observed levels. This can be attributed to the fact these states are mainly described by the coupling of the ground state of ^{90}Zr with a single neutron at $h_{11/2}$. ii) our calculation reproduces an additional $11/2^+$ at 2.61 MeV. It would be a very useful test for our calculation a more extended experimental investigation for the existence or not of such a state. iii) A possible $1/2^-$ state at 2.35 MeV is predicted by our calculation 1 MeV higher. If the existence of such a state is confirmed then the good agreement between theory and experiment could be partially destroyed. iv) In the spectrum of ^{91}Zr all the high spin states above 2.5 MeV like the $21/2^+$, $13/2^-$ and $17/2^+$ are reproduced to within 300 KeV. Finally as we can see observing the spectrum of ^{93}Mo our calculation accounts satisfactorily for all the observed levels¹⁹) as well as all the high spin states that are above 2.5 MeV. All the possible high spin states above 2.5 MeV are reproduced to within 100-200 KeV.

The experimental information on the electromagnetic decay of the $N = 51$ nuclei is limited and for this reason the most of the experimental data shown in table 3 are only estimates. There are some interesting features to be observed in the calculation of the transition probabilities. As we can see in table 3, four out of five B(M1) probabilities in the spectrum of ^{92}Nb , are in disagreement with the experimental estimations. One should note that the experimental B(M1) values are very small quantities. This indicates that even a small change in the wavefunctions of these states could improve the agreement between theory and experiment. The same feature can be observed in the M1 transition $9/2^+ \rightarrow 7/2^+$ of ^{93}Mo . It is worth noting also that on the transition $3^- \rightarrow 2^-$ of ^{90}Y which is a mixture of M1 and E2 there is an experimental estimate for the M1 transition but not for the corresponding E2. However the multipole mixing ratio $\delta(E2/M1)$ for this particular transition has been measured and its value is $\delta = -0.04 \pm 0.04$. The calculated value for this quantity is -0.03 , which is in very good agreement with the experimental data. Similary results we have for the transition $7^+ \rightarrow 3^-$ of ^{90}Y which is a mixture of E5 and M4. The calculated value of δ which is 5.3×10^{-3} lies within the experimental estimate. Generally as may be observed in this table, there is a good agreement of the theory predictions with the experimental data. Such a feature certainly increases the confidence on the validity of the model employed in the calculation.

Table 3
Reduced Transition Probabilities B(QL) in the $N = 51$, $39 \leq Z \leq 46$ nuclei

QL	Nucl	$J_i^{\pi*}$	E_i^\dagger	$J_f^{\pi*}$	E_f^\dagger	Exper [‡]	Calc	
M1	⁹⁴ Tc	6 ⁺	102	7 ⁺	0		0.68	
		5 ⁺	210	6 ⁺	102		0.65	
	⁹³ Mo	7 ⁺	1363	5 ⁺	0	$(6.8 \pm 0.6) \times 10^{-2}$	7×10^{-2}	
		9 ⁺	1477	7 ⁺	1363	$(27 \pm 13) \times 10^{-5}$	0.04	
		7 ⁺	1520	5 ⁺	0		0.10	
		5 ⁺	1695	7 ⁺	1363	0.56 ± 0.06	0.14	
		13 ⁻	2450	11 ⁻	2440	0.7	0.04	
	⁹² Nb	3 ⁺	285	2 ⁺	135	$(5 \pm 3) \times 10^{-3}$	0.78	
		3 ⁻	389	2 ⁻	225	> 0.0004	0.03	
		4 ⁺	480	5 ⁺	357	$(4.4 \pm 0.9) \times 10^{-3}$	1.00	
		6 ⁺	501	7 ⁺	0	$(5 \pm 8) \times 10^{-4}$	0.43	
		4 ⁺	480	3 ⁺	285	$(3.4 \pm 0.6) \times 10^{-3}$	1.65	
	⁹¹ Zr	7 ⁺	1882	5 ⁺	0	0.022^{+10}_{-19}	0.13	
		5 ⁺	1466	5 ⁺	0	$(37 \pm 18) \times 10^{-3}$	44×10^{-3}	
		3 ⁺	2042	5 ⁺	0	0.23 ± 0.02	0.80	
		7 ⁺	2200	5 ⁺	0	$(48 \pm 26) \times 10^{-4}$	34×10^{-4}	
	⁹⁰ Y	15 ⁻	2287	13 ⁻	2259	$(34 \pm 13) \times 10^{-3}$	42×10^{-3}	
		3 ⁻	205	2 ⁻	0	$(102 \pm 3) \times 10^{-4}$	136×10^{-4}	
	E2	⁹⁴ Tc	6 ⁺	102	7 ⁺	0		4.45
			5 ⁺	210	6 ⁺	102		0.15
⁹⁵ Ru		17 ⁺	2284	13 ⁺	2029	6.4 ± 0.6	0.95	
		21 ⁺	2539	17 ⁺	2284	1.94 ± 0.05	1.12	
⁹³ Mo		7 ⁺	1363	5 ⁺	0	8.7 ± 2.4	4.62	
		9 ⁺	1477	5 ⁺	0	12 ± 4	8.02	
		9 ⁺	1477	7 ⁺	1363		0.97	
		7 ⁺	1520	5 ⁺	0		6.42	
		13 ⁺	2161	9 ⁺	1477	3.6 ± 0.3	4.88	
17 ⁺		2429	13 ⁺	2161	4.64 ± 0.24	2.20		

*For odd mass nuclei the value quoted corresponds to 2J

†In KeV

‡In Weisskopf units

Table 3
Continued

QL	Nucl	$J_i^{\pi^*}$	E_i^\dagger	$J_f^{\pi^*}$	E_f^\dagger	Exper [†]	Calc
E2	⁹² Nb	3 ⁺	285	2 ⁺	135	1.2±0.9	3.84
		5 ⁺	357	7 ⁺	0	2.03±0.05	1.42
		3 ⁻	389	2 ⁻	225	> 0.16	0.96
		4 ⁺	480	5 ⁺	357	0.6±0.7	0.49
		11 ⁻	2203	9 ⁻	2080	3.92±0.11	2.60
	⁹¹ Zr	1 ⁺	1204	5 ⁺	0	54±19	5.48
		7 ⁺	1882	5 ⁺	0	6 ⁺⁶ ₋₃	11.5
		3 ⁺	2042	5 ⁺	0	60±5	1.75
		9 ⁺	2131	5 ⁺	0	4.4±0.7	5.46
		7 ⁺	2200	5 ⁺	0	0.9±0.5	0.50
⁹⁰ Y	3 ⁻	205	2 ⁻	0		0.21	
M3	⁹⁶ Rh	3 ⁺	52	6 ⁺	0	1.49±0.14	1.07
E3	⁹¹ Zr	11 ⁻	2170	5 ⁺	0		4.79
		21 ⁺	3167	15 ⁻	2288	(5.4±0.6) × 10 ⁻²	0.44
M4	⁹⁰ Y	7 ⁺	682	3 ⁻	202	1.58±0.05	4.01
E4	⁹² Mo	21 ⁺	2424	13 ⁺	2161	1.45±0.01	0.03
E5	⁹⁰ Y	7 ⁺	682	3 ⁻	202		1.68
		7 ⁺	682	2 ⁻	0	1.75±0.16	2.47

References

- [1] I. Talmi and I. Unna, Nucl. Phys. **19** (1960) 225
- [2] G.M. Gazzally, N.M. Hintz, M.A. Franey, J. Dubach and W.C. Haxton Phys. Rev. **C28** (1983) 294
- [3] W.C. Haxton and D. Strottman unpublished
- [4] X. Ji and B.H. Wildenthal Phys. Rev. **C37** (1988) 1256
- [5] X. Ji and B.H. Wildenthal Phys. Rev. **C38** (1988) 2849
- [6] X. Ji and B.H. Wildenthal Phys. Rev. **C40** (1988) 389
- [7] J. Sinatkas, L.D. Skouras, D. Strottman and J.D Vergados Phys. G: Nucl. Part. Phys. **18** (1992) 1377
- [8] J. Sinatkas, L.D. Skouras, D. Strottman and J.D Vergados Phys. G: Nucl. Part. Phys. **18** (1992) 1401
- [9] J. Sinatkas, L.D. Skouras and J.D. Vergados Phys. Rev. **C37** (1988) 1229
- [10] L.D. Skouras and D. Manakos Phys. G: Nucl. Part. Phys. **19** (1993) 731
- [11] L.D. Skouras and C. Dedes Phys. Rev. **C15** (1977) 1873
- [12] P. Divari and L.D. Skouras A study of the $N = 51$ nuclei, to be published
- [13] J.P. Elliot, A.D. Jackson, H.A. Mavromatis, E.A. Sanderson and B. Singh Nucl. Phys. **A121** (1968) 241
- [14] B. Haesner and P. Luksch Nucl. Data Sheets **46** (1985) 718
- [15] T.W. Burrows Nucl. Data Sheets **68** (1993) 720
- [16] M. Coral Nucl. Data Sheets **66** (1992) 400
- [17] J.K. Tuli Nucl. Data Sheets **66** (1992) 53
- [18] H.-W. Muller Nucl. Data Sheets **60** (1990) 854
- [19] H. Sievers Nucl. Data Sheets **54** (1988) 160